Supporting Information for:

Electronic and Nuclear Structural Snapshots in Ligand Dissociation and Recombination Processes of Iron Porphyrin in Solution: A Combined Optical/X-ray Approach

Michael W. Mara[1,2], Andrew Stickrath[2], Megan Shelby[1], Mike Harpham[2], Jier Huang[2], Xiaoyi Zhang[2,3],Brian M. Hoffman[1], and Lin X. Chen[1,2]*

[1]Department of Chemistry, Northwestern University, 2145 Sheridan Road, Evanston, Illinois 60208-3113; [2]Chemical Sciences and Engineering Division and [3]X-ray Sciences Division of the Advanced Photon Source, Argonne National Laboratory, 9700 South Cass Avenue, Argonne, Illinois 60439

RECEIVED DATE (automatically inserted by publisher); E-mail: lchen@anl.gov or l-chen@northwestern.edu

*Corresponding Author contact information:

E-mail: lchen@anl.gov or l-chen@northwestern.edu;

Phone: 630-252-3533 or 847-491-3479.

S1. Determination of Excited-State Fraction in Time-Resolved XAFS Measurements

Since 100 % excitation by the pump laser is generally not achieved in transient experiments, it is necessary to remove the ground-state contribution from the transient spectra. The dynamics of the ligand recombination to the iron porphyrin are expected to involve the independent binding of two imidazole ligands, followed by recombination of the carbon monoxide on the microsecond time scale. Once the hexa-coordinate complex is formed with two axial imidazole ligands, the main dynamic expected is conversion from this hexa-coordinated complex to the ground state complex which has both an imidazole and a carbon monoxide ligands, which appears to be observed beginning with the 3.6 μs spectrum. Therefore, the transient spectra S_{sig} from this time delay on can be treated with the following equation:

$$S_{sig} = f_{GS}S_{GS} + f_{ES}S_{ES}$$

where S and f are the spectra and fraction contributions of the spectra, respectively. Therefore, S_{ES} is easily extracted once f_{GS} and f_{ES} are determined.

According to the dynamic scheme presented, an XAFS spectrum of ground state iron porphyrin in 30% v/v 1-methylimidazole/water was obtained while under N_2 purge instead of CO purge. In this case, the excited-state spectra from 3.6 μs on can be treated as a linear combination of the ground-state spectrum (CO still bound) and the no-CO spectrum. The plots of the 3.6 μs plot (before ground-state subtraction), FePP-CO, and FePP, as well as the results from the LCA fits, are shown in Figures S1A and S1B, respectively. The linear combination fits match the data quite well, with some minor differences at the peak of the white line, most likely due to differences in normalization between the two standard spectra. The *FePP-CO spectrum fits best to 65.5% FePP-CO and 34.5% FePP.

S2. Fourier-Transform of FePP Spectrum

Following photoexcitation, metal-bound porphyrins exhibit picoseconds vibrational relaxation, followed by rebinding of photodissociated ligands bound axially to the metal center. At longer time delays, it is expected that the significant dynamics observed will belong simply to the ligand recombination. CO tends to exhibit minimal geminate recombination; therefore, the dynamics on the microsecond time scale will likely correspond to replacing one of the axial ligands with CO. Im tends to bind very strongly to iron, and so it is likely that on the microsecond time scale, an iron porphyrin with two axially-bound Im ligands will be observed. FePP, an iron protoporphyrin IX in the absence of CO, is likely to form such a structure and therefore was considered an accurate model for *FePP-CO at all time delays following the 100 ps time delay spectrum; therefore, the XAFS spectrum of FePP in 30% v/v Im/H_2O was obtained.

The energy space, k-space, and R-space spectra of *FePP-CO at 3.6 μs and FePP are shown in Figure S2. The XANES shows similar features in each spectrum; namely, a strong pre-edge peak at 7112.8 eV, likely corresponding to $1s \rightarrow 3d_{x2-y2}$ and $3d_{z2}$ transitions, and weaker, broader transitions on the edge. The spectra show roughly the same spectral features in k-space. R-space fits for FePP are shown in Figure S3; the XAFS parameters are in Table S1, along with those for *FePP-CO at 3.6 μs. There is a large difference in the magnitude of the R-space peaks between the two spectra, which is likely due to the difference in signal-to-noise at high k between the two data sets. The two samples exhibit some minor differences in Fe-C_α and Fe-C_β distance. However, both still best match a model consisting of two Im bound axially to the Fe. The 1.98-1.99 Å distance between the Fe center and the nearest atomic neighbors is also consistent with ligation of two Im; while another proposed structure would replace one or both

Im with water molecules, due to the ~10:1 H_2O:Im ratio, the nearest neighbor distance is much shorter than that exhibited commonly for systems involving an Fe(II) atom bound to H_2O. While there are some minor differences in the R-space spectra between these two samples, they appear to represent essentially the same structure. It also seems clear that this system consists of two axially-bound Im, with no appreciable amount of H_2O directly bound to Fe.

S3. Transient Absorption Kinetic Traces

The XTA measurements performed have a time resolution of 80-100 ps, and therefore are unable to measure the initial ligand dynamics and vibrational relaxation that occur on the 10s of picoseconds time scales. Transient absorption measurements were performed using a 415 nm excitation pulse to probe the dynamics that occur faster than the XTA response time. Kinetics traces at 530 nm and 585 nm are shown in Figure S4. Both kinetic traces exhibit an ~3 ps lifetime that is consistent with vibrational cooling that is present in photoexcited iron porphyrin systems.[1] The Q-bands were observed to red-shift ~20 ps following photoexcitation, which is consistent with the binding of the 1st axial ligand measured in previous iron porphyrin TA measurements. The 585 nm kinetics also exhibit a 20 ps decay lifetime, consistent with the formation of the triplet porphyrin excited state $^3T(\pi,\pi^*)$.[2]

S4. XAFS Scattering Paths

Plots of all XAFS scattering paths used in the fits of FePP-CO and *FePP-CO at 100 ps and 3.6 μs delays are shown in imaginary FT space in Figures S5a, b, and c, respectively. Multiple scattering paths involving both the N's of the porphyrin ring and C_α and C_β were also included. Also, additional multiple scattering paths were included for *FePP-CO at 3.6 μs, which accounted for scattering involving the N's of the two bound Im ligands. Multiple scattering contributions should be included in XAFS data analysis since their interference with single

scattering paths can influence the total magnitude of the signal in R-space, and are therefore necessary to properly model the spectrum. In this case, the Fe-C_α-N paths are largely out of phase with the Fe-C_m paths and therefore destructively interfere; the same is true of the Fe-C_m-N paths and the Fe-C_β paths. As a result, the peaks in the FT corresponding to these paths become washed out, broadening the peaks and decreasing their magnitude. It should also be noted that the difference in magnitude and shape of the first shell peak in the FT of ground state FePP-CO is due to destructive interference between the Fe-C(CO) and Fe-N scattering paths. As a result, the magnitude of the first shell peak for FePP-CO is lower than that of *FePP-CO at 100 ps, despite the larger coordination number of FePP-CO.

References

(1) Franzen, S.; Kiger, L.; Poyart, C.; Martin, J.-L. Heme Photolysis Occurs by Ultrafast Excited State Metal-to-Ring Charge Transfer. *Biophys. J.* **2001**, *80*, 2372-2385.

(2) Dixon, D. W.; Kirmaier, C.; Holten, D. Picosecond Photodissociation of Six-coordinate Iron(II) Pporphyrins. *J. Am. Chem. Soc.* **1985**, *107*, 808-813.

Figures

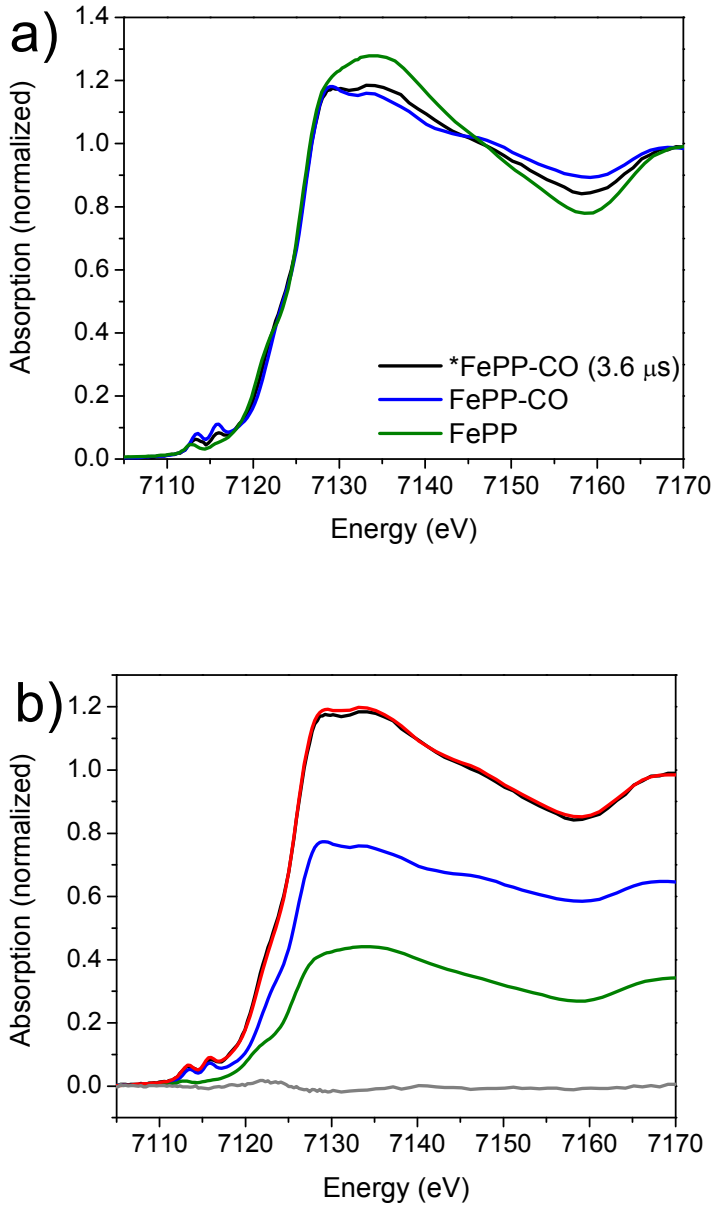

Figure S1: a) XANES spectra of *FePP-CO at 3.6 μs delay (black), FePP-CO (blue), and FePP (green). b) Linear combination fit using 65.5% FePP-CO and 34.5% FePP. Fit shown in red and difference between spectrum and fit shown in gray.

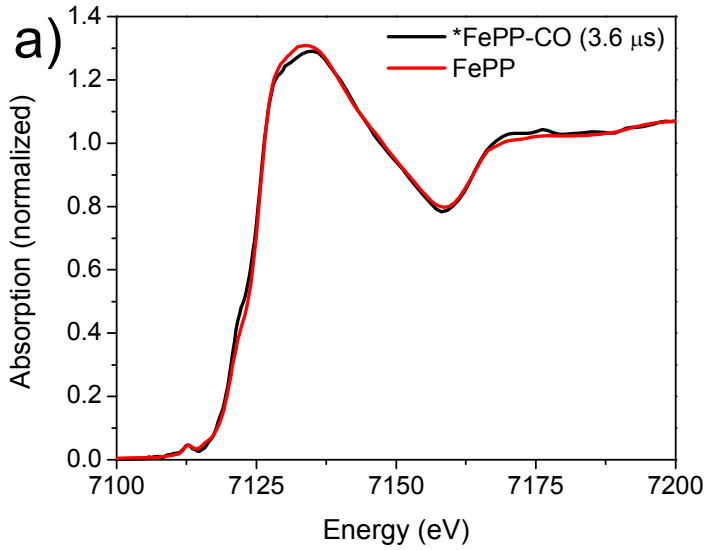
a)
*FePP-CO (3.6 μs)
FePP
Absorption (normalized)
Energy (eV)
1.4
1.2
1.0
0.8
0.6
0.4
0.2
0.0
7100
7125
7150
7175
7200

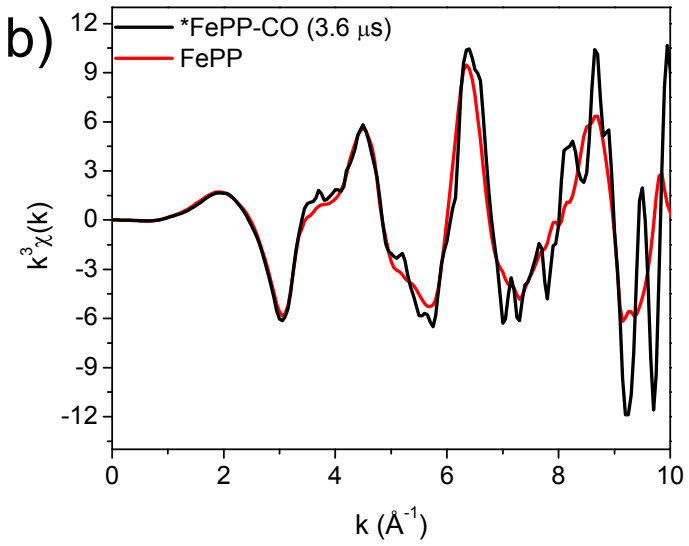
b)
*FePP-CO (3.6 μs)
FePP
k³χ(k)
k (Å⁻¹)
12
9
6
3
0
-3
-6
-9
-12
0
2
4
6
8
10

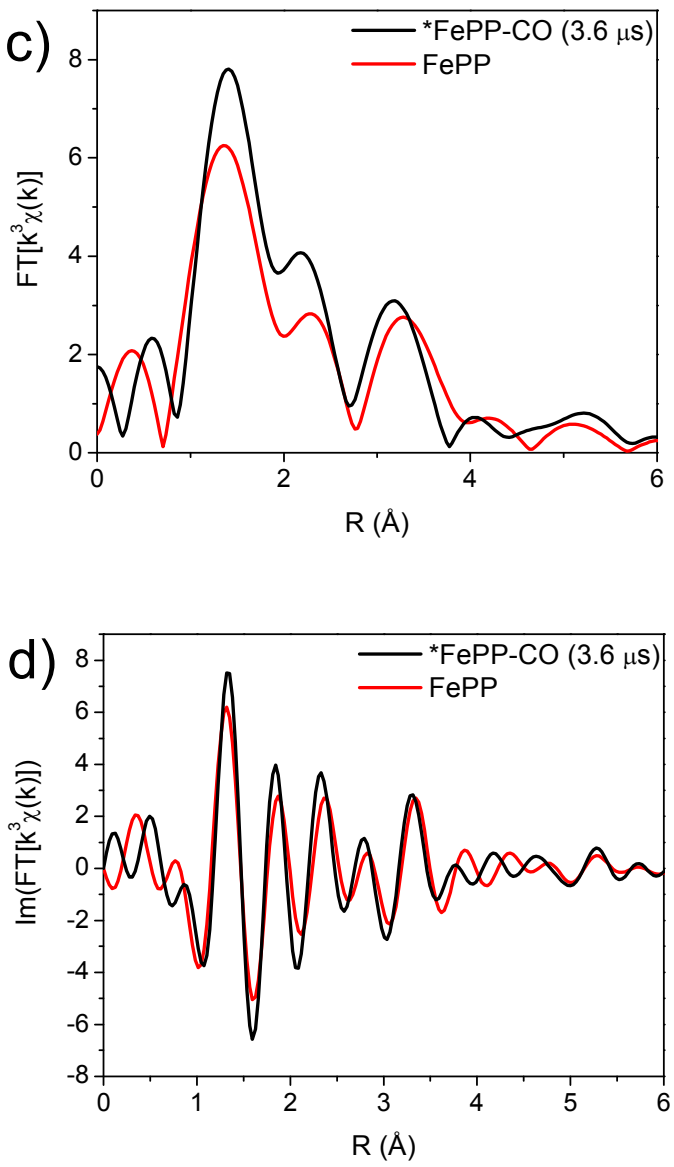

Figure S2: Energy space (a), k-space (b), magnitude R (c), and imaginary R (d) plots of *FePP-CO at 3.6 μs delay (black) and FePP (red). Fourier transform range was 2.5 – 8 $Å^{-1}$

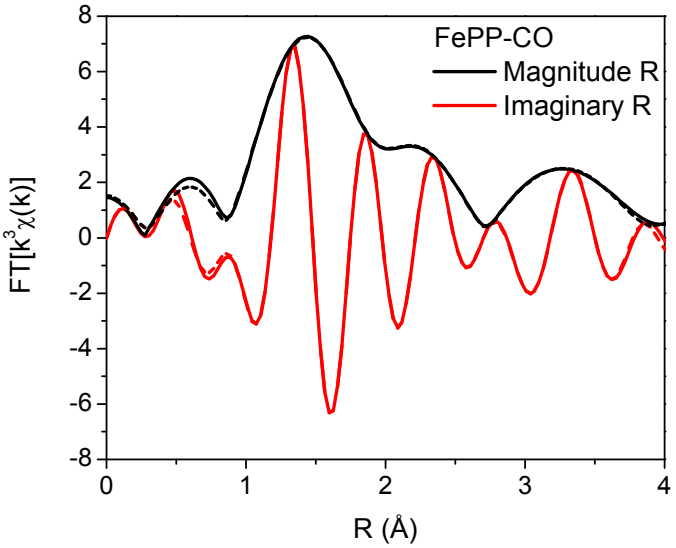

Figure S3: Magnitude (black) and Imaginary (red) R-space fits for FePP. Data shown as solid line, fit as dashed line

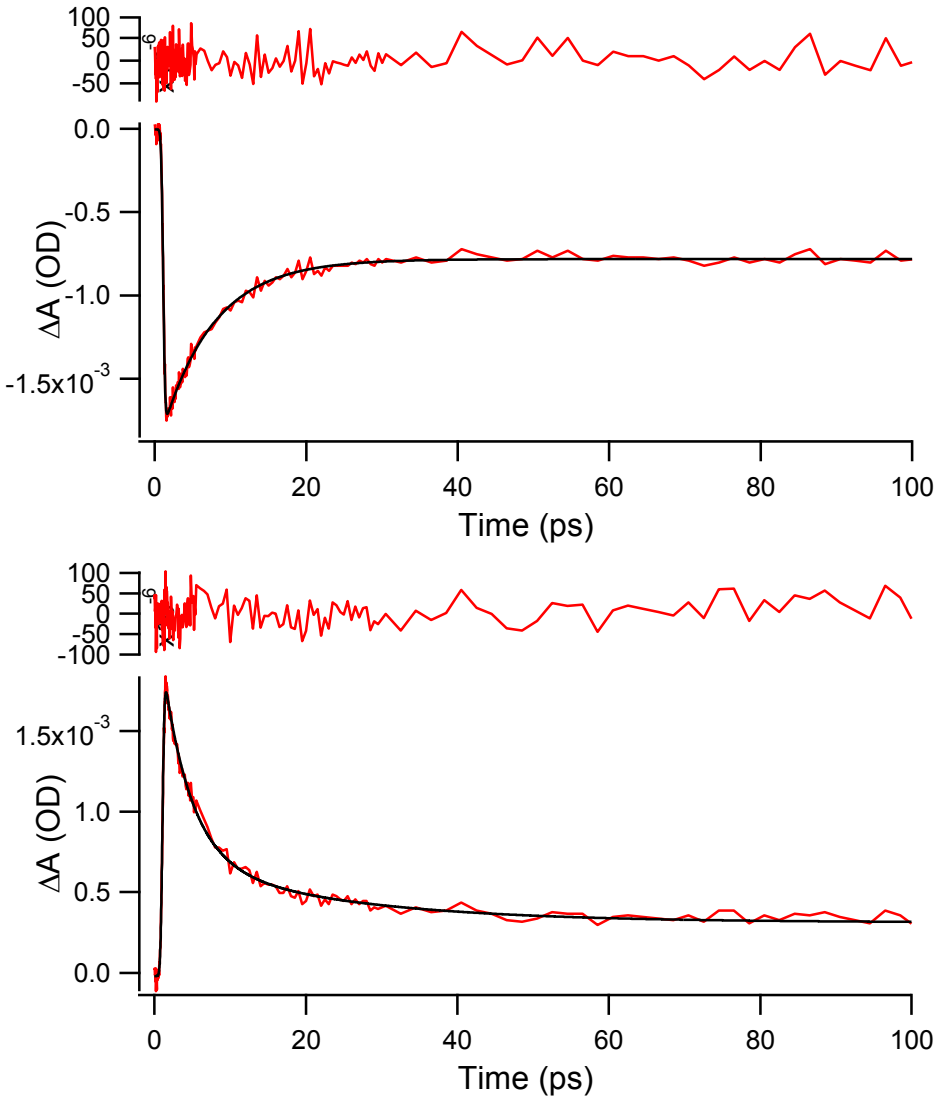

Figure S4: Transient absorption kinetic traces at 530 nm (top) and 585 nm (bottom). Residual is shown above each data plot.

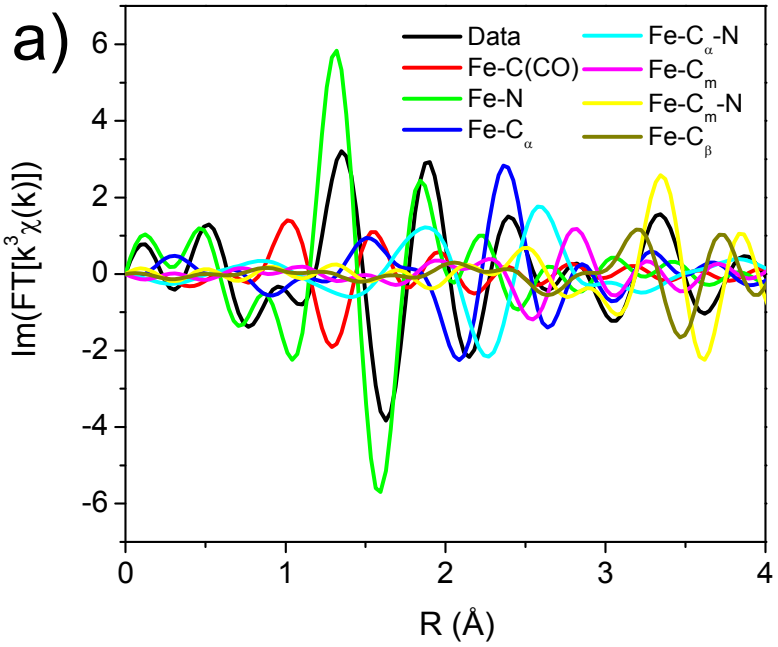
a)
Data
Fe-C(CO)
Fe-N
Fe-Cα
Fe-Cα-N
Fe-Cm
Fe-Cm-N
Fe-Cβ
Im(FT[k3χ(k)])
R (Å)

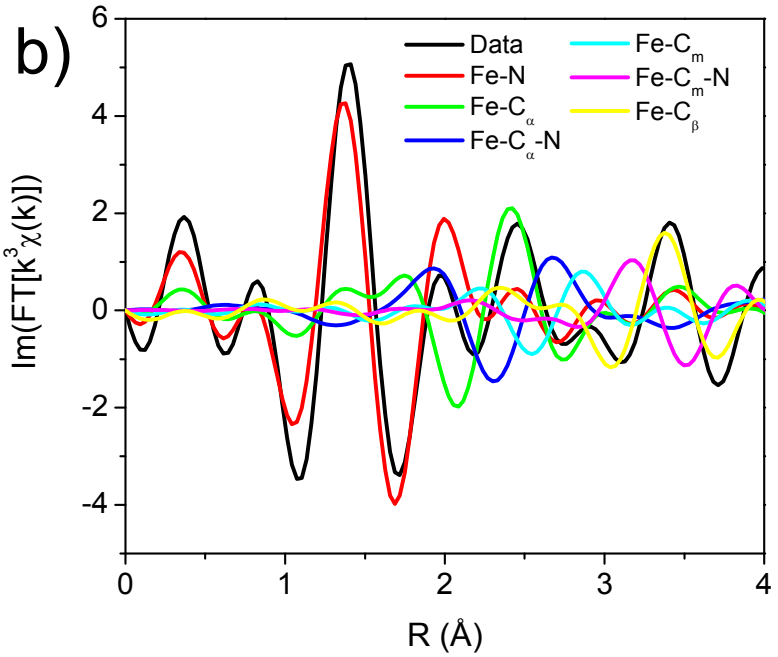
b)
Data
Fe-N
Fe-Cα
Fe-Cα-N
Fe-Cm
Fe-Cm-N
Fe-Cβ
Im(FT[k3χ(k)])
R (Å)

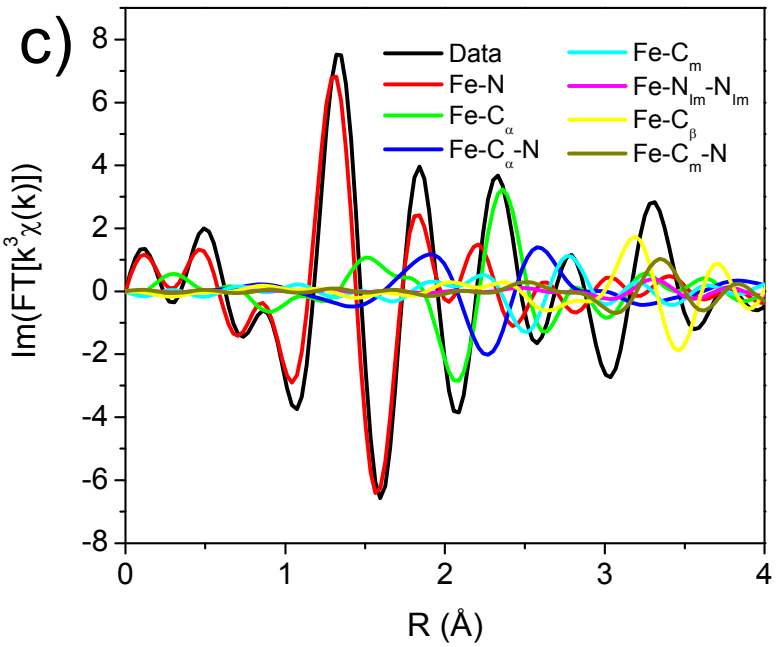

Figure S5: XAFS scattering paths used in the data fitting of FePP-CO (a) and *FePP-CO and 100 ps (b) and 3.6 μs (c) time delays. Multiple scattering paths included in fits are also shown, displaying interference between single scattering and multiple scattering paths

Table S1: *FePP-CO (3.6 µs) and FePP XAFS Parameters – S_0^2 = 0.9							
*FePP-CO (3.6 µs): ΔE = -0.47 eV				FePP: ΔE = 3.50 eV			
Path	CN	R (Å)	σ^2 (Å^2)	Path	CN	R (Å)	σ^2 (Å^2)
Fe-N	6	1.98	0.003	Fe-N	6	1.99	0.003
Fe-C_α	12	2.95	0.003	Fe-C_α	12	2.99	0.004
Fe-C_m	4	3.39	0.001	Fe-C_m	4	3.40	0.001
Fe-C_β	12	4.33	0.001	Fe-C_β	12	4.35	0.006